

PAPER

Automatic high order aberrations correction for digital holographic microscopy based on orthonormal polynomials fitting over irregular shaped aperture

Recent citations

- [Dingnan Deng *et al*](#)

To cite this article: Zhongming Yang *et al* 2019 *J. Opt.* **21** 045609

View the [article online](#) for updates and enhancements.




IOP | ebooks™

Bringing you innovative digital publishing with leading voices to create your essential collection of books in STEM research.

Start exploring the collection - download the first chapter of every title for free.

Automatic high order aberrations correction for digital holographic microscopy based on orthonormal polynomials fitting over irregular shaped aperture

Zhongming Yang¹ , Zhaojun Liu¹, Weilin He¹, Jiantai Dou², Xin Liu¹ and Chao Zuo³

¹School of Information Science & Engineering and Shandong Provincial Key Laboratory of Laser Technology and Application, Shandong University, Qingdao 266237, People's Republic of China

²Department of Physics, College of Science, Jiangsu University of Science and Technology, 2 Mengxi Road, Zhenjiang, Jiangsu 212003, People's Republic of China

³Institute of Electrical Engineering & Photoelectric Technology, Nanjing University of Science & Technology, Nanjing, Jiangsu, 210094, People's Republic of China

E-mail: zhaojunliu@sdu.edu.cn

Received 11 February 2019

Accepted for publication 8 March 2019

Published 22 March 2019



CrossMark

Abstract

We propose an automatic high-order aberration correction method for digital holographic microscopy based on orthonormal polynomial fitting over an irregular-shaped aperture. The corner detection technique is used to detect the specimen-free area for orthonormal polynomials over an irregular-shaped aperture. The high-order aberration correction method is completely automatic and requires only a single hologram. Experiments showed that in aberration correction, both lower-order phase curvatures and high-order aberrations could be corrected without requiring extra devices. Numerical simulations show that the proposed method provides more accurate high-order aberration correction than aberration correction methods based on least squares fitting with standard polynomials. Experimental results demonstrate the feasibility of using the proposed method for analyzing human macrophage cells.

Keywords: digital holography, aberration compensation, interference microscopy, phase measurement

1. Introduction

Digital holographic microscopy (DHM) is an interferometric, nondestructive, label-free technique for acquiring quantitative phase images. Thus far, it has been used in applications such as cell biology analysis [1], particle tracking [2], microfluidics metrology [3], and neural science [4]. In DHM, the object wave transmitted or reflected from a specimen is collected by a microscope objective to enhance the spatial resolution. However, aligning the microscope objective is often difficult in a laboratory, and the phase aberrations introduced by this misalignment are superposed over the phase information induced by the specimen.

Compensating for this phase aberration is critical in both DHM and digital holographic microtomography. In recent years, various physical and numerical methods have been proposed to address this issue. Physical methods include double exposure [5], position-adjustable lens [6], and the same objective lens in a reference wave [7]. However, these methods usually require precise alignment. To overcome this challenge, many numerical compensation methods have been proposed. Principal component analysis and optimal principal component analysis have been used to extract the spherical phase curvature for digital holography; however, they are not applicable to high-order aberrations [8, 9]. Spectral analysis methods have been used to acquire the degrees of phase aberrations;

however, the sampling interval in the Fourier domain limits the aberrations correction accuracy [10, 11]. In least squares fitting methods, phase aberrations are fitted using standard polynomials [12], spherical surface [13], parabolic function [14], or Zernike polynomials [15]; however, a specimen-free area must be selected for fitting. Recently, deep learning techniques with convolutional neural networks have been used for selecting a specimen-free area for Zernike polynomial fitting [16]. A nonlinear optimization procedure has also been used for phase aberration extraction [17]. However, for the specimen-free area, orthonormal polynomials are neither orthogonal nor represent classical aberrations. To the best of our knowledge, almost all aberration corrections for DHM based on least squares fitting methods cannot remove the fitting error introduced by the loss of orthogonality of standard orthonormal polynomials, especially for high-order aberration correction for DHM and digital holographic microtomography.

This paper presents a high-order aberration correction method based on orthonormal polynomials fitted over an irregular-shaped aperture for a transmission DHM system with the Michelson interferometric configuration. The corner detection technique is used to detect the specimen-free area for orthonormal polynomials over an irregular-shaped aperture. The high-order aberration correction method is completely automatic and requires only a single hologram. Simulation results for human macrophage cells demonstrate the validity of this method.

2. Principle

The specimen-free area in holograms usually has an irregular-shaped aperture, and the fitting error introduced by the loss of orthogonality of standard orthonormal polynomials can be superposed over the specimen. Based on Zernike polynomials over a unit circular aperture, polynomials that are orthogonal over noncircular apertures such as annular [18], hexagonal [19], elliptical [20], rectangular [21], square [22], and olivary [23] apertures are obtained through orthogonalization. Recently, we have developed expressions for orthogonal polynomials over irregular-shaped apertures that are used for absolute measurements of optical surface figures [24, 25]. The orthogonalization process is described briefly here.

Zernike polynomials $Z_n^m(\rho, \theta)$ are widely used in optical testing and wavefront analysis for their orthogonality over a unit circular aperture, which can represent classical aberrations in an optical system. They can be written as [26]

$$\begin{cases} Z_n^m(\rho, \theta) = \left[\frac{2(n+1)}{1+\delta_{m0}} \right]^{\frac{1}{2}} R_n^m(\rho) \cos(m\theta) \\ R_n^m(\rho) = \sum_{s=0}^{(n-m)/2} \frac{(-1)^s (n-s)!}{s! \left(\frac{n+m}{2} - s\right)! \left(\frac{n-m}{2} - s\right)!} \rho^{n-2s} \end{cases} \quad (1)$$

where (ρ, θ) is the polar coordinate over the unit circular aperture, n and m are positive integers including 0 and

$n - m > 0$, and δ_{ij} is the Kronecker delta. The Zernike polynomials are orthogonal over a unit circular aperture as given by

$$\begin{cases} \frac{1}{\pi} \int_0^1 \int_0^{2\pi} Z_n^m(\rho, \theta) Z_{n'}^{m'}(\rho, \theta) \rho d\rho d\theta = \delta_{mm'} \delta_{nn'} \\ \int_0^{2\pi} \cos(m\theta) \cos(m'\theta) d\theta = \pi(1 + \delta_{m0}) \delta_{mm'} \\ \int_0^1 R_n^m(\rho) R_{n'}^m(\rho) \rho d\rho = \frac{1}{2(n+1)} \delta_{nn'} \end{cases} \quad (2)$$

In a DHM system, the phase aberrations $W(\rho, \theta)$ containing discrete data points over a unit circular aperture can be expanded in terms of Zernike polynomials $Z_i(\rho, \theta)$:

$$W(\rho, \theta) = \sum_{i=1}^N c_i Z_i(\rho, \theta), \quad (3)$$

where Z_i is the Zernike polynomial of the i th term and N is the total number of terms in the Zernike polynomial. The Zernike expansion coefficients c_i are given by

$$c_i = \frac{1}{\pi} \int_0^1 \int_0^{2\pi} W(\rho, \theta) Z_i(\rho, \theta) \rho d\rho d\theta. \quad (4)$$

However, the specimen-free area in holograms usually has an irregular-shaped aperture, Zernike polynomials are neither orthogonal nor represent classical aberrations. If we use the terms of Zernike polynomials representing the phase aberrations $W(\rho, \theta)$ based on equation (4), the accuracy and stability of the calculation procedure of c_i greatly degrade and the data sets with an irregular-shaped aperture seriously deviate from a unit circular aperture. To obtain orthogonal polynomials over general aperture shapes, studies have used Gram–Schmidt orthogonalization [18–25]. In Gram–Schmidt orthogonalization, the Zernike polynomials $Z_i(\rho', \theta')$ can be expanded by the orthogonal polynomials $F_i(\rho', \theta')$ over general aperture shapes. The Zernike polynomials $Z_i(\rho', \theta')$ and conversion coefficient α are given by equation (5)

$$\begin{cases} Z_i(\rho', \theta') = \sum_{k=1}^i \alpha_{ki} F_k(\rho', \theta') \\ \alpha_{ki} = \begin{cases} \sum [Z_i(\rho', \theta') F_k(\rho', \theta')], & k < i \\ \left\{ \sum [Z_i(\rho', \theta')]^2 - \sum_{k=1}^{i-1} \alpha_{ki}^2 \right\}^{1/2}, & k = i \end{cases} \end{cases} \quad (5)$$

where (ρ', θ') is the polar coordinate over the irregular-shaped aperture and the orthogonal polynomials over general aperture shapes $F_i(\rho', \theta')$ can be expressed as

$$F_i(\rho', \theta') = \frac{1}{\alpha_{ii}} \left[Z_i(\rho', \theta') - \sum_{k=1}^{i-1} \alpha_{ki}^2 F_k(\rho', \theta') \right]. \quad (6)$$

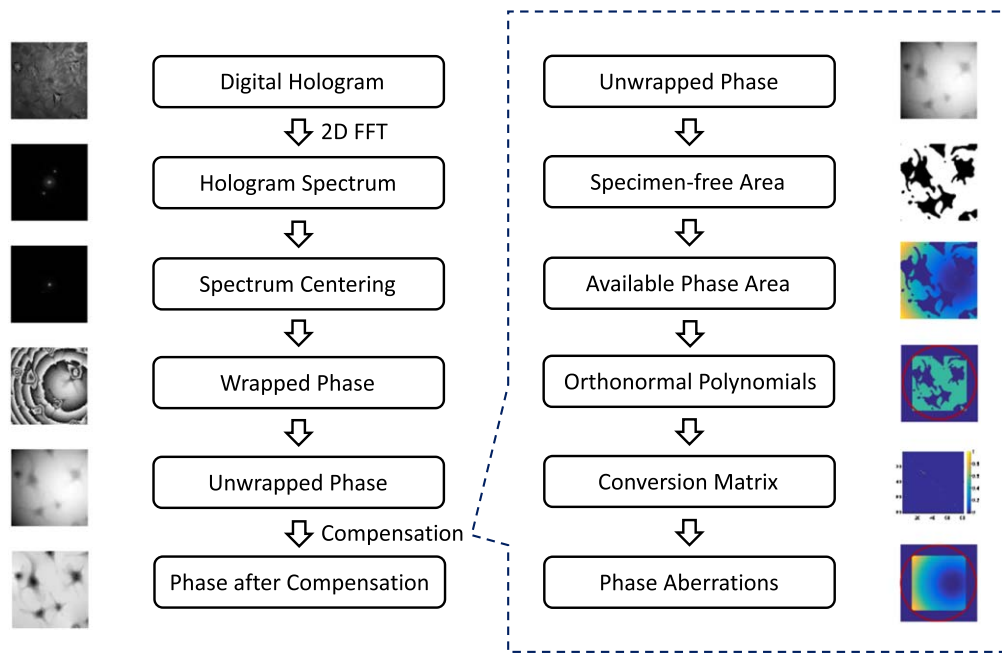


Figure 1. Block diagram of phase reconstruction of traditional DHM and proposed automatic high-order aberration correction algorithm.

Therefore, phase aberrations $W(\rho', \theta')$ that measure discrete data points over general aperture shapes can be expanded in terms of $F_k(\rho', \theta')$ and the coefficients a_k can be expressed as

$$\left\{ \begin{aligned} W(\rho', \theta') &= \sum_{k=1}^N a_k F_k(\rho', \theta') = \sum_{i=1}^N c_i Z_i(\rho', \theta') \\ &= \sum_{j=1}^N c_j \left[\sum_{k=1}^i \alpha_{kj} F_k(\rho', \theta') \right] \\ a_k &= \sum_{i=k}^N c_i \alpha_{ki} \end{aligned} \right. \quad (7)$$

Utilizing the orthogonality property of orthogonal polynomials $F_k(\rho', \theta')$, orthogonal polynomials expansion coefficients a_k can be expressed as

$$a_k = \iint_{(\rho', \theta') \in D} W(\rho', \theta') F_k(\rho', \theta') \rho' d\rho' d\theta', \quad (8)$$

where D is the specimen-free area in holograms. The Zernike expansion coefficients c_i can be expressed as

$$c = \alpha^{-1} a. \quad (9)$$

Based on the Zernike expansion coefficients c_i , the phase aberrations $W(\rho, \theta)$ over a unit circular aperture in DHM can be calculated by equation (4).

Figure 1 shows a block diagram of the phase reconstruction of traditional DHM and the steps in our automatic high-order aberration correction method for DHM based on orthonormal polynomials fitted over an irregular-shaped aperture. Just like phase aberration correction methods based on least squares fitting, the phase aberrations are fitted by standard polynomials and we need to select a specimen-free area for fitting. A machine learning corner detection approach

has been proposed to automatically determine the specimen-free area based on an unwrapped phase [27]. Then, we can obtain the available phase background region that allows for orthonormal polynomial fitting. After expanding the background region of a specimen-free area to a unit circular aperture, the orthonormal polynomials are calculated through orthogonalization. The coefficients of orthogonal polynomials over general aperture shapes a_k are given by equation (9). Based on the conversion matrix of Zernike polynomial coefficients and orthogonal polynomial coefficients, Zernike expansion coefficients over a unit circular aperture can be calculated. Just like the Zernike polynomials used in wavefront analysis, quantitative analysis of high-order aberrations is performed using specimen-free phase data. Finally, high-order phase aberrations in DHM are compensated.

3. Simulation

To validate the feasibility of the proposed high-order aberration correction method, we used previously reported specimen phase data [8] in our numerical simulation. Figure 2(a) shows the specimen phase data after removing the phase map in the specimen-free area over a unit circular aperture, and figure 2(b) shows the mask of the specimen-free area. The phase aberrations in DHM are generated from the sum of 81-term Zernike polynomials, as shown in figure 3(a). The Zernike polynomials are usually used to represent classical aberrations in the optical system. Figure 3(b) shows the coefficients of the Zernike polynomials of the phase aberrations.

Figure 4(a) shows a simulated phase image of the specimen with the phase aberration in the numerical simulation, which is the sum of the specimen phase data and the phase

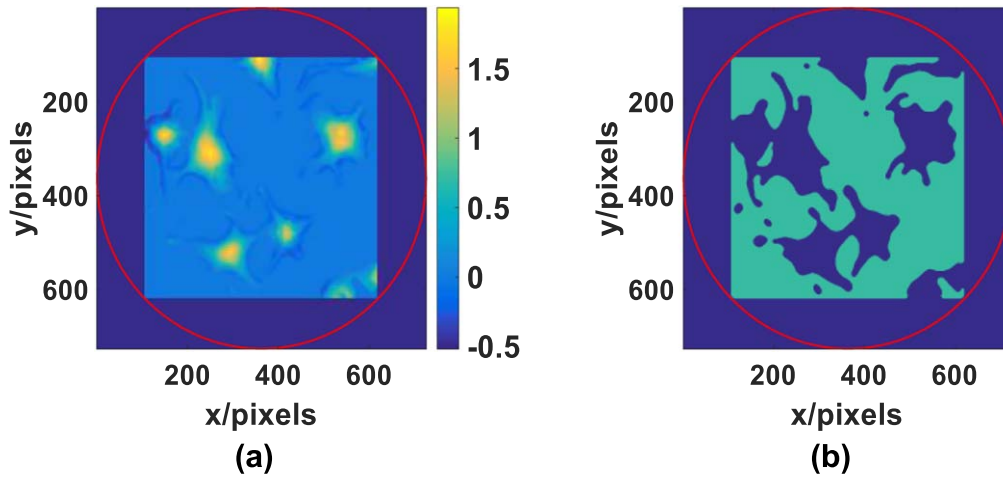


Figure 2. Specimen phase data over a unit circular aperture in numerical simulation. (a) Specimen phase data after removing the phase map in the specimen-free area and (b) the mask of the specimen-free area.

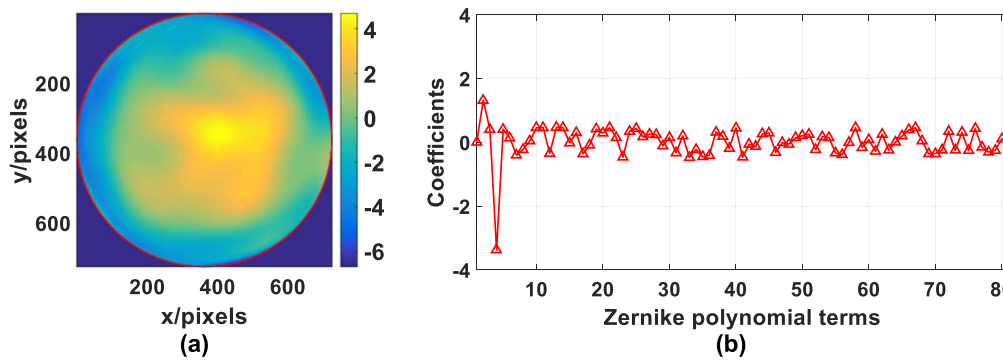


Figure 3. Phase aberrations in the numerical simulation. (a) Phase aberrations are generated by the sum of 81-term Zernike polynomials, and (b) coefficients of Zernike polynomials of phase aberrations.

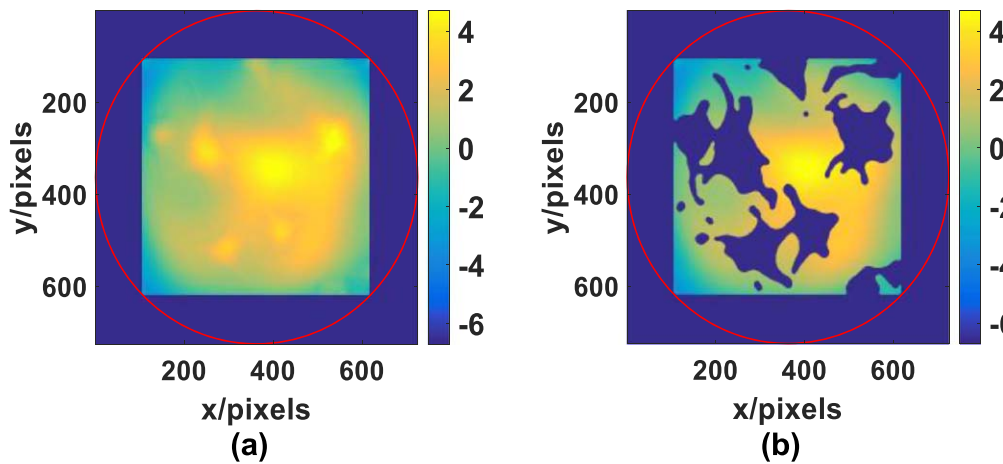


Figure 4. Phase image of specimen with phase aberration in the numerical simulation. (a) Phase image of specimen with the phase aberration and (b) specimen-free area selected for fitting.

aberrations over a unit circular aperture. Figure 4(b) shows the selected specimen-free area for orthonormal polynomial fitting. Figure 5 shows the compensation result obtained with the Zernike polynomial fitting method in the numerical simulation and the corrected phase aberrations. Figure 6 shows a comparison of the Zernike polynomial coefficients of

the simulated and the corrected phase aberrations. This figure indicates that low-order phase aberrations have been corrected partially, whereas high-order phase aberrations cannot be corrected by traditional Zernike polynomial fitting.

Based on the phase aberration correction procedure, the orthonormal polynomial coefficients of simulated phase

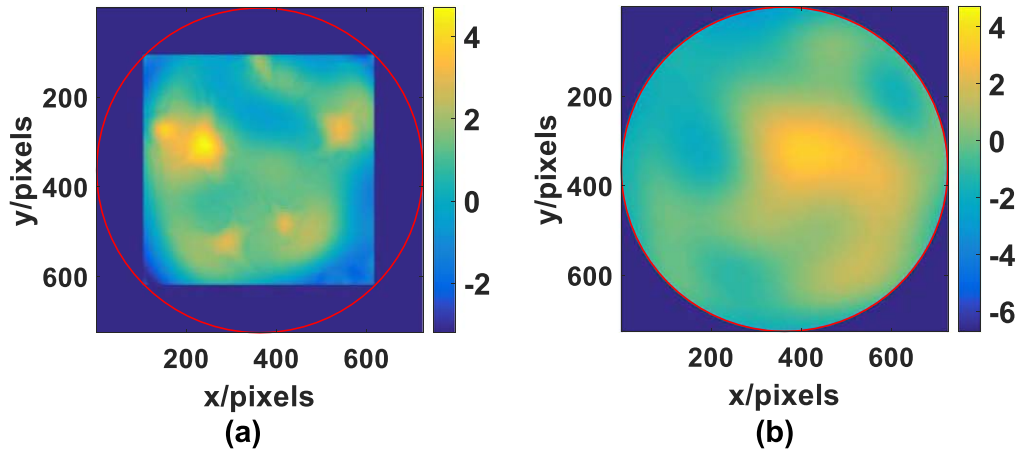


Figure 5. Compensation result obtained with Zernike surface fitting method in the numerical simulation. (a) Compensation result and (b) corrected phase aberrations.

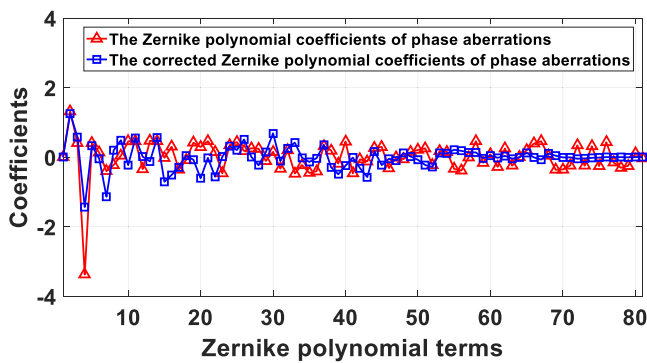


Figure 6. Comparison of Zernike polynomial coefficients of simulated and corrected phase aberrations obtained by the Zernike polynomial fitting method.

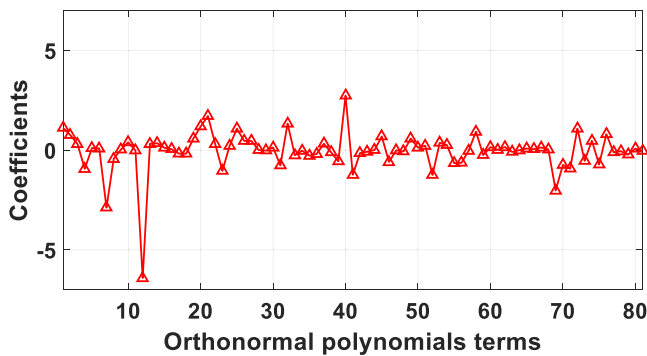


Figure 7. Orthonormal polynomial coefficients of simulated phase aberrations obtained by the proposed orthonormal polynomial fitting method.

aberrations obtained by the proposed orthonormal polynomials fitting method are shown in figure 7, and the conversion coefficient matrix for Gram–Schmidt orthogonalization is shown in figure 8. Figure 9 shows the compensation result obtained using the orthonormal polynomial fitting method in the numerical simulation and the corrected phase aberrations. Figure 10(a) shows a comparison of the Zernike polynomial coefficients of the simulated and the corrected phase

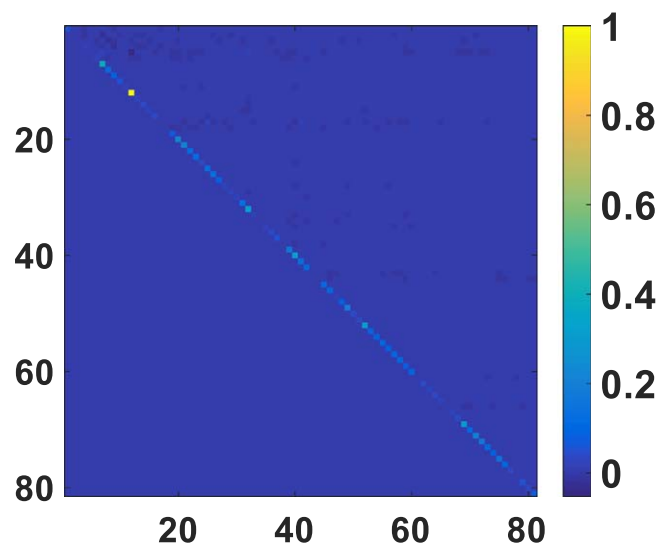


Figure 8. Conversion coefficient matrix for Gram–Schmidt orthogonalization.

aberrations, figure 10(b) shows the deviation distribution of the results from the initial assumed phase aberrations, with the $PV = 3.13 \times 10^{-14} \lambda$ and $rms = 2.37 \times 10^{-14} \lambda$. This figure indicates that low- and high-order phase aberrations have been corrected by our proposed orthonormal polynomial fitting over an irregular-shaped aperture.

4. Experiments

To verify the automatic high-order aberration correction method based on orthonormal polynomial fitting over an irregular-shaped aperture, experimental results for human macrophage cells are shown in figure 11(a), and a reconstructed phase map of a hologram without phase aberration compensation over a unit circular aperture is shown in figure 11(b). The phase map in figure 11(b) shows significant defocusing and spherical aberration. Based on the phase reconstruction of DHM and the proposed automatic high-order aberration

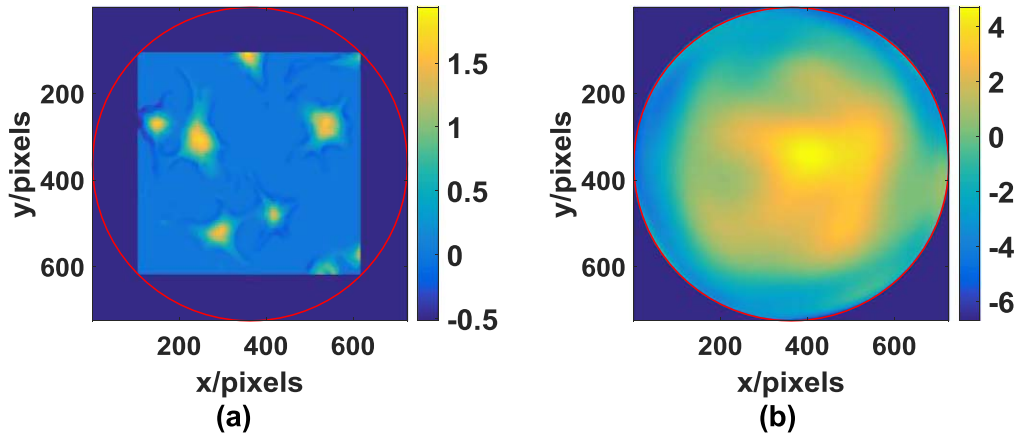


Figure 9. Compensation result obtained using the orthonormal polynomial fitting method over an irregular-shaped aperture in the numerical simulation. (a) Compensation result and (b) corrected phase aberrations.

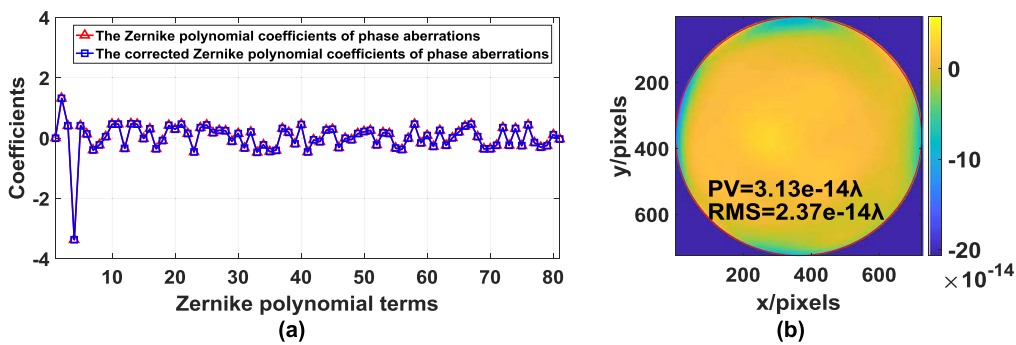


Figure 10. The simulation results. (a) Comparison of Zernike polynomial coefficients of simulated and corrected phase aberrations obtained by the orthonormal polynomial fitting method and (b) the deviation distribution of the results from the initial assumed phase aberrations.

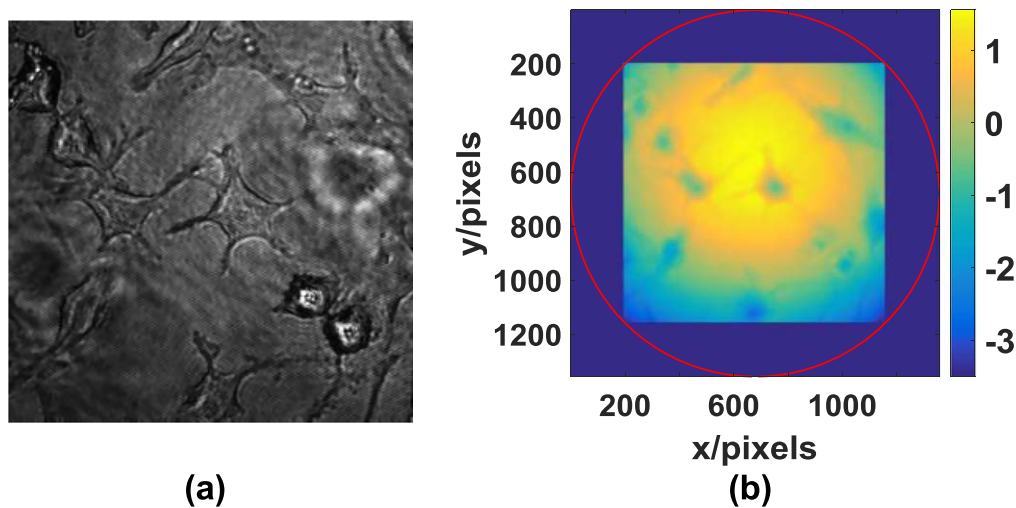


Figure 11. Experimental results on human macrophage cells without aberration correction. (a) Digital hologram and (b) reconstructed phase map without phase aberration compensation over a unit circular aperture.

correction methods, as shown in figure 1, the mask of the specimen-free area is shown in figure 12(a) and the reconstructed phase map over the specimen-free area is shown in figure 12(b). Figure 13(a) shows the corrected results obtained using the Zernike polynomial fitting method, and figure 13(b) shows the compensated phase aberrations. Figure 14(a) shows

the corrected results obtained using the orthonormal polynomial fitting method over an irregular-shaped aperture, and figure 14(b) shows the compensated phase aberrations. The results and improvements from figures 13(a) and 14(a) seem mostly minor and achievable with a changed contrast rather than with aberrations correction, but the phase aberration has

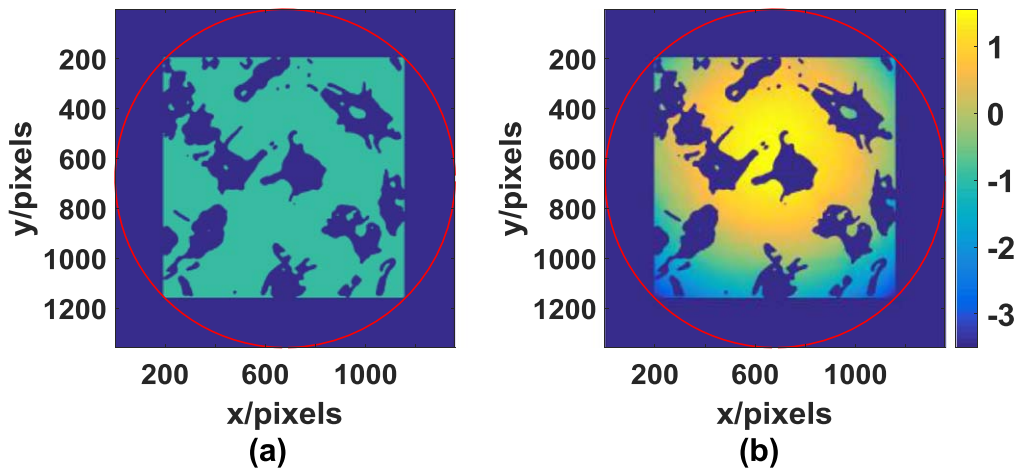


Figure 12. Reconstructed phase map over the specimen-free area without phase aberration compensation. (a) Mask of the specimen-free area and (b) reconstructed phase map over the specimen-free area.

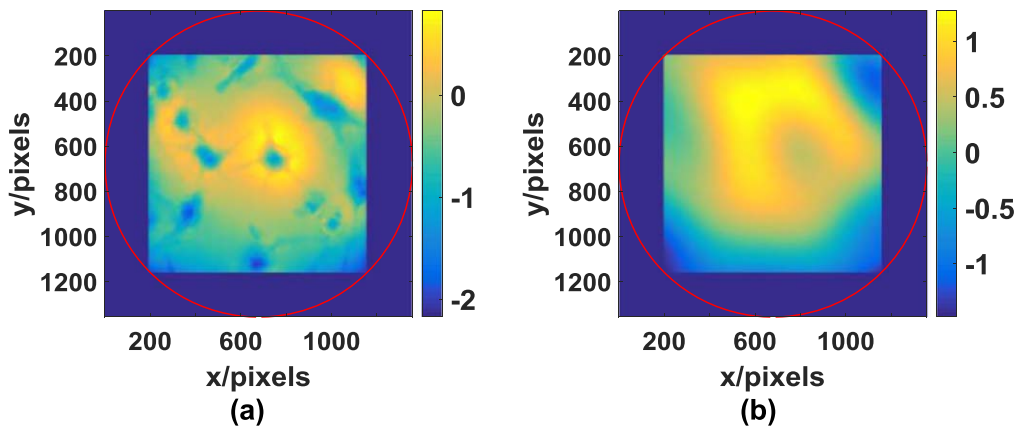


Figure 13. Corrected results obtained using the Zernike polynomial fitting method. (a) Corrected results and (b) compensated phase aberrations.

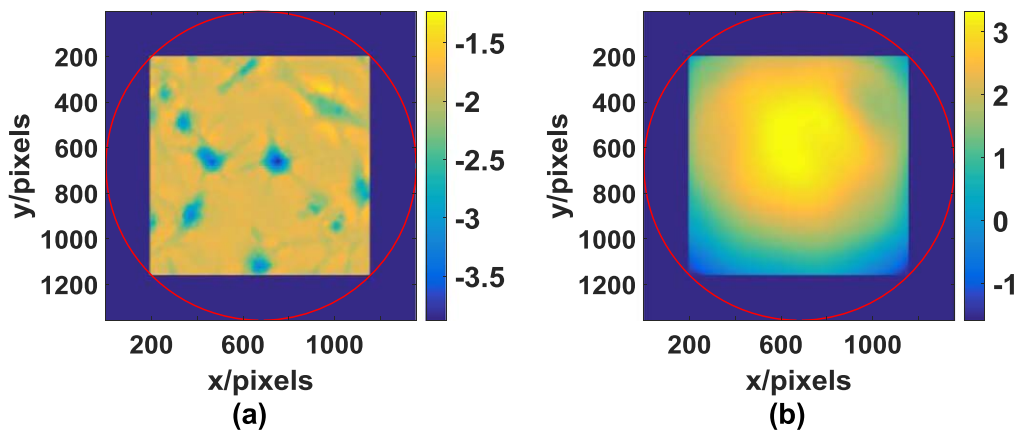


Figure 14. Corrected results obtained using the orthonormal polynomial fitting method over an irregular-shaped aperture. (a) Corrected results and (b) compensated phase aberrations.

been corrected. Figure 15 shows a comparison of the results obtained using the Zernike polynomial fitting method and the orthonormal polynomial fitting method over an irregular-shaped aperture. The corrected results obtained using the latter

method indicate that high-order phase aberrations have been corrected, and they have the same order of magnitude as lower-order phase aberrations. In our automatic high-order aberration correction for DHM, the calculation time is 1.1 min, which

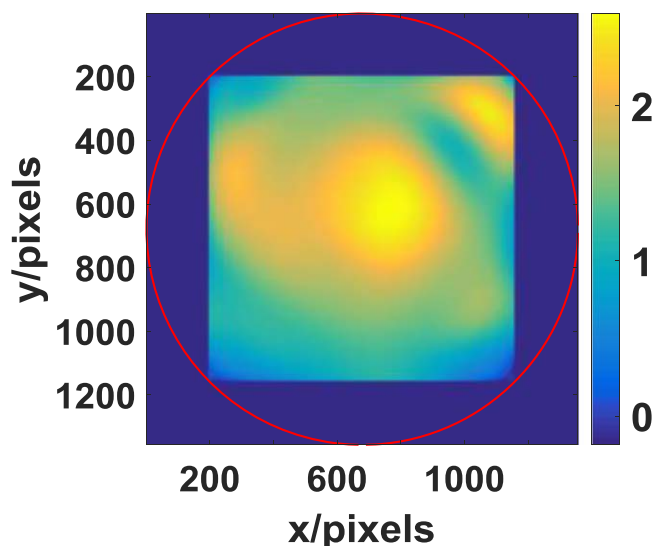


Figure 15. Comparison of the results obtained using the Zernike polynomial fitting method and orthonormal polynomial fitting method over an irregular-shaped aperture.

depends on the Gram–Schmidt orthogonalization procedure over irregular-shaped aperture and the size of the digital hologram. In the experiment, all calculations are performed on a laptop with a 2.4GHz i7 CPU and 8G RAM using MATLAB®.

5. Conclusion

We have presented a high-order aberration correction method for DHM based on orthonormal polynomial fitting over an irregular-shaped aperture. The corner detection technique is used to detect the specimen-free area for the orthonormal polynomials over an irregular-shaped aperture. Compared with the traditional phase aberration correction method, our proposed aberration correction method can correct low- and high-order phase aberrations. Our aberration correction method is completely automatic and requires only a single hologram. These characteristics make it a very effective tool for DHM.

Acknowledgments

We would like to thank the China Postdoctoral Science Foundation (2018M630773), the Research Supported by the Opening Project of CAS Key Laboratory of Astronomical Optics & Technology, Nanjing Institute of Astronomical Optics & Technology (CAS-KLAOT-KF201804), and Fundamental Research Funds of Shandong University (11170077614092) for financial support.

ORCID iDs

Zhongming Yang  <https://orcid.org/0000-0002-2146-5021>

References

- [1] Kühn J et al 2002 Label-free cytotoxicity screening assay by digital holographic microscopy *ASSAY Drug Dev. Technol.* **11** 101–7
- [2] Warnasooriya N, Joud F, Bun P, Tessier G, Coppey-Moisand M, Desbiolles P, Atlan M, Abboud M and Gross M 2002 Imaging gold nanoparticles in living cell environments using heterodyne digital holographic microscopy *Opt. Express* **18** 3264–73
- [3] John R and Pandiyan P 2016 An optofluidic bio-imaging platform for quantitative phase imaging of lab on a chip devices *Appl. Opt.* **55** 54–9
- [4] Pavillon N, Benke A, Boss D, Moratal C, Kühn J, Jourdain P, Depeursinge C, Magistretti P J and Marquet P 2002 Cell morphology and intracellular ionic homeostasis explored with a multimodal approach combining epifluorescence and digital holographic microscopy *J. Biophoton.* **3** 432–6
- [5] Ferraro P, De Nicola S, Finizio A, Coppola G, Grilli S, Magro C and Pierattini G 2002 Compensation of the inherent wave front curvature in digital holographic coherent microscopy for quantitative phase-contrast imaging *Appl. Opt.* **42** 1938–46
- [6] Qu W, Choo C O, Singh V R, Yingjie Y and Asundi A 2002 Quasi-physical phase compensation in digital holographic microscopy *J. Opt. Soc. Am. A* **26** 2005–11
- [7] Mann C J, Yu L, Lo C-M and Kim M K 2002 High-resolution quantitative phase-contrast microscopy by digital holography *Opt. Express* **13** 8693–8
- [8] Zuo C, Chen Q, Qu W and Asundi A 2002 Phase aberration compensation in digital holographic microscopy based on principal component analysis *Opt. Lett.* **38** 1724–6
- [9] Sun J, Chen Q, Zhang Y and Zuo C 2002 Optimal principal component analysis-based numerical phase aberration compensation method for digital holography *Opt. Lett.* **41** 1293–6
- [10] Cui H, Wang D, Wang Y, Zhao J and Zhang Y 2002 Phase aberration compensation by spectrum centering in digital holographic microscopy *Opt. Commun.* **284** 4152–5
- [11] Liu S, Xiao W and Pan F 2002 Automatic compensation of phase aberrations in digital holographic microscopy for living cells investigation by using spectral energy analysis *Opt. Laser Technol.* **57** 169–74
- [12] Colomb T, Cuche E, Charrière F, Kühn J, Aspert N, Montfort F, Marquet P and Depeursinge C 2002 Automatic procedure for aberration compensation in digital holographic microscopy and applications to specimen shape compensation *Appl. Opt.* **45** 851–63
- [13] Di J, Zhao J, Sun W, Jiang H and Yan X 2002 Phase aberration compensation of digital holographic microscopy based on least squares surface fitting *Opt. Commun.* **282** 3873–7
- [14] Min J, Yao B, Ketelhut S, Engwer C, Greve B and Kemper B 2017 Simple and fast spectral domain algorithm for quantitative phase imaging of living cells with digital holographic microscopy *Opt. Lett.* **42** 227–30
- [15] Miccio L, Alfieri D, Grilli S, Ferraro P, Finizio A, De Petrocellis L and Nicola S D 2002 Direct full compensation of the aberrations in quantitative phase microscopy of thin objects by a single digital hologram *Appl. Phys. Lett.* **90** 041104
- [16] Nguyen T, Bui V, Lam V, Raub C B, Chang L-C and Nehmetallah G 2002 Automatic phase aberration compensation for digital holographic microscopy based on deep learning background detection *Opt. Express* **25** 15043–57
- [17] Liu S, Lian Q, Qing Y and Xu Z 2002 Automatic phase aberration compensation for digital holographic microscopy based on phase variation minimization *Opt. Lett.* **43** 1870–3

- [18] Mahajan V N and Díaz J A 2002 Imaging characteristics of Zernike and annular polynomial aberrations *Appl. Opt.* **52** 2062–74
- [19] Mahajan V N and Dai G-m 2002 Orthonormal polynomials for hexagonal pupils *Opt. Lett.* **31** 2462–4
- [20] Díaz J A and Navarro R 2002 Orthonormal polynomials for elliptical wavefronts with an arbitrary orientation *Appl. Opt.* **53** 2051–7
- [21] Azimipour M, Atry F and Pashaie R 2002 Calibration of digital optical phase conjugation setups based on orthonormal rectangular polynomials *Appl. Opt.* **55** 2873–80
- [22] Ye J, Gao Z, Wang S, Cheng J, Wang W and Sun W 2002 Comparative assessment of orthogonal polynomials for wavefront reconstruction over the square aperture *J. Opt. Soc. Am. A* **31** 2304–11
- [23] Zheng Y, Sun S and Li Y 2002 Zernike olivary polynomials for applications with olivary pupils *Appl. Opt.* **55** 3116–25
- [24] Ye J, Wang W, Gao Z, Liu Z, Wang S, Benítez P, Miñano J C and Yuan Q 2002 Modal wavefront estimation from its slopes by numerical orthogonal transformation method over general shaped aperture *Opt. Express* **23** 26208–20
- [25] Du J, Yang Z, Liu Z and Fan G 2002 Three-step shift-rotation absolute measurement of optical surface figure with irregular shaped aperture *Opt. Commun.* **426** 589–97
- [26] Malacara D 2007 *Optical Shop Testing* (New York: Wiley)
- [27] Rosten E, Porter R and Drummond T 2002 Faster and better: a machine learning approach to corner detection *IEEE Trans. Pattern Anal. Mach. Intell.* **32** 105–19